FULL-LENGTH ORIGINAL RESEARCH

Determinants of brain metabolism changes in mesial temporal lobe epilepsy

*†‡§Francine Chassoux, ¶**Eric Artiges, ††Franck Semah, §‡‡Serge Desarnaud, *†‡Agathe Laurent, *†Elisabeth Landre, §‡‡Philippe Gervais, *†Bertrand Devaux, and §‡‡Ourkia Badia Helal

Epilepsia, **(*):1–13, 2016
doi: 10.1111/epi.13377

Francine Chassoux is a neurologist, who heads the Epilepsy Unit at Sainte-Anne Hospital in Paris.

Summary

Objective: **To determine the main factors influencing metabolic changes in mesial temporal lobe epilepsy (MTLE) due to hippocampal sclerosis (HS).**

Methods: **We prospectively studied 114 patients with MTLE (62 female; 60 left HS; 15- to 56-year-olds) with ^{18}F-fluorodeoxyglucose–positron emission tomography and correlated the results with the side of HS, structural atrophy, electroclinical features, gender, age at onset, epilepsy duration, and seizure frequency. Imaging processing was performed using statistical parametric mapping.**

Results: **Ipsilateral hypometabolism involved temporal (mesial structures, pole, and lateral cortex) and extratemporal areas including the insula, frontal lobe, perisylvian regions, and thalamus, more extensively in right HS (RHS). A relative increase of metabolism (hypermetabolism) was found in the nonepileptic temporal lobe and in posterior areas bilaterally. Voxel-based morphometry detected unilateral hippocampus atrophy and gray matter concentration decrease in both frontal lobes, more extensively in left HS (LHS). Regardless of the structural alterations, the topography of hypometabolism correlated strongly with the extent of epileptic networks (mesial, anterior-mesiolateral, widespread mesiolateral, and bitemporal according to the ictal spread), which were larger in RHS. Notably, widespread perisylvian and bitemporal hypometabolism was found only in RHS. Mirror hypermetabolism was grossly proportional to the hypometabolic areas, coinciding partly with the default mode network. Gender-related effect was significant mainly in the contralateral frontal lobe, in which metabolism was higher in female patients. Epilepsy duration correlated with the contralateral temporal metabolism, positively in LHS and negatively in RHS. Opposite results were found with age at onset. High seizure frequency correlated negatively with the contralateral metabolism in LHS.**

Significance: **Epileptic networks, as assessed by electroclinical correlations, appear to be the main determinant of hypometabolism in MTLE. Compensatory mechanisms reflected by a relative hypermetabolism in the nonepileptic temporal lobe and in extratemporal areas seem more efficient in LHS and in female patients, whereas long duration, late onset of epilepsy, and high seizure frequency may reduce these adaptive changes.**

KEY WORDS: **Mesial temporal lobe epilepsy, Hippocampal sclerosis, Metabolism, PET, Epileptic networks.**

Accepted March 7, 2016.

*Department of Neurosurgery, Sainte-Anne Hospital, Paris, France; †Paris Descartes University, Paris, France; ‡INSERM U 1129, Paris, France; §Department of Nuclear Medicine, SHFJ, CEA, Orsay, France; ¶INSERM U 1000, Paris, France; **Psychiatry Department 91G16, Orsay Hospital, Paris Descartes University, Orsay, France; ††Department of Nuclear Medicine, INSERM U 1171, University Hospital of Lille, Lille, France; and ‡‡INSERM U 1023 IMIV, CEA, Paris-Sud University, Orsay, France

Address correspondence to Francine Chassoux, Unité d'Epileptologie Clinique Chirurgicale, Centre Hospitalier Sainte-Anne, 1, rue Cabanis, 75014 Paris, France. E-mail f.chassoux@ch-sainte-anne.fr

Key Points

- Epileptic networks assessed by electroclinical features appear the main determinant of hypometabolism in MTLE
- Extratemporal hypometabolism, especially in the perisylvian areas, is more extensive on the right side, regardless of the structural alterations
- Gender, epilepsy duration, age at onset, and seizure frequency all contributed to some intergroup differences; however, none of these factors appears to account for the variability of ipsilateral hypometabolism
- Contralateral temporal and bilateral posterior hypermetabolism coincide partly with the areas involved in the default mode network

Brain metabolism assessed by ^{18}F-fluorodeoxyglucose–positron emission tomography (^{18}F-FDG-PET) has been studied in mesial temporal lobe epilepsy (MTLE) associated with hippocampal sclerosis (HS) for >30 years, allowing localization and lateralization of the epileptic focus. However, despite an overall characteristic hypometabolic pattern, its topography is highly variable at the individual level. Determinants of metabolic changes have been related to multiple factors, such as hippocampal volume, neuronal loss, decrease of synaptic activity and density, and ictal symptomatology.[1–3] We demonstrated previously that hypometabolism correlated with the extent of epileptic networks, characterized by the ictal-onset zone and spread pathways, including a gradual involvement of the insular and perisylvian regions.[4,5] According to these data, imaging and neurophysiologic studies all point to the fact that MTLE is not a focal but rather a network disease that can affect interconnected, even remote, structures throughout the brain.[6,7] Furthermore, structural and functional imaging data provide evidence that MTLE is a progressive disease.[8–13] Several studies have also brought to light asymmetric changes in the cortex, the white matter and brain connectivity, depending on the side of the affected hemisphere.[14–16] Previous PET studies had already suggested that the consequences of epilepsy may differ according to epilepsy lateralization and gender.[2,17–19] However, most of these confounding factors have been studied separately, using an asymmetry index obtained from preselected regions of interest (ROIs), or based on relatively limited cohorts pooling right and left hemispheres.

We aimed to study a large cohort of patients in whom right and left MTLE would be analyzed separately in male and female participants, using a whole brain statistical parametric analysis. Our goal was to determine which factor(s) mainly influence(s) the extent of metabolic changes in temporal and extratemporal areas. We postulated that epileptic networks would be the major determinants of brain hypometabolism, after controlling for the effects of other variables such side of HS, structural atrophy, gender, duration of the disease, age at epilepsy onset, and seizure frequency.

Patients and Methods

We prospectively studied 114 consecutive patients with drug-resistant MTLE and unilateral HS (60 left [LHS], 54 right [RHS]; 62 female; 15- to 56-year-olds) between 2002 and 2012, following and distinct from a previously reported cohort (Table 1).[4] Surgery was performed in 100 patients, with neuropathologic confirmation of HS in all cases. Among patients with at least a 2-year follow-up (n = 96), 88% obtained seizure-free outcome.

Informed consent was obtained from all subjects. The protocol was approved by the local ethics committee. Presurgical workup consisted of electroencephalography (EEG)–video monitoring, neuropsychological testing, magnetic resonance imaging (MRI), Wada test, and/or functional MRI in all patients and stereo-EEG in 13 patients. Electroclinical patterns were defined as described previously[4] and classified into the following four groups according to the propagation of ictal discharges. The Mesial group deals with very focal (intralobar) seizures characterized by short duration, incomplete/inconstant loss of consciousness, simple automatisms, no or brief postictal confusion/language deficit, no secondary tonic–clonic generalization (STCG), anterior temporal localized spikes and ictal discharge. The Anterior Mesial-Lateral (AML) group corresponds to anterior (insulofrontal) propagation characterized by a secondary complete loss of consciousness, more complex automatisms, dystonic posturing, head deviation, delayed somatomotor manifestations and salivation, postictal confusion/language deficit, possible STCG, regional (temporofrontal) spikes, and anterior spread of ictal discharge. The Widespread Mesial-Lateral (WML) group—for widespread (perisylvian) propagation—differs from the AML group by early loss of consciousness, salivation, somatomotor manifestations and head/eye version, prolonged postictal confusion/language deficit, frequent STCG, widespread temporal spikes diffusing to frontocentral/parietal areas, and hemispheric ictal discharge. The Bitemporal (BT) group—for contralateral temporal propagation—is defined by early loss of consciousness, prolonged and massive postictal confusion/language deficit, bilateral asynchronous temporal spikes, and bitemporal discharge. The type of aura was not discriminant.

Image acquisition and processing

^{18}F-FDG-PET was performed interictally using a high-resolution head-dedicated PET camera (Siemens-Exact HR+, Knoxville, TN, U.S.A.) providing 63 slices (intrinsic in-plane resolution: 4.3 mm; voxel size: 2.42 × 2.42 × 2.43 mm^3). All patients were injected and scanned at rest in

Table 1. Clinical characteristics of the population

	RHS (n = 54)	LHS (n = 60)	Total (n = 114)	p-Value
Gender F/M	24/30	38/22	62/52	0.04
Age at time of study years, min-max (mean ± SD)				
Female	15–47 (29.7 ± 10.1)	15–56 (33.4 ± 12.1)	15–56 (31.9 ± 11.4)	0.79
Male	15–56 (32.9 ± 9.4)	16–45 (29.6 ± 8.3)	15–56 (31.5 ± 9)	
Total	15–56 (31.5 ± 9.8)	15–56 (32 ± 10.9)	15–56 (31.8 ± 10.4)	
Age at epilepsy onset years, min-max (mean ± SD)				
Female	2–30 (10.1 ± 6.9)	2–40 (10.4 ± 9.7)	2–40 (10.3 ± 8.7)	0.88 (0.21)*
Male	1–26 (12.3 ± 8.1)	4–30 (12.1 ± 6.4)	1–30 (12.2 ± 7.3)	
Total	1–30 (11.3 ± 7.6)	2–40 (11.1 ± 8.7)	1–40 (11.2 ± 8.1)	
Epilepsy duration years, min-max (mean ± SD)				
Female	4–36 (19.6 ± 8.6)	2–53 (22.9 ± 13.4)	2–53 (21.6 ± 11.8)	0.71 (0.9)*
Male	5–41 (20.6 ± 11.4)	4–34 (17.5 ± 8.7)	4–41 (19.3 ± 10.4)	
Total	4–41 (20.2 ± 10.2)	2–53 (21 ± 10.1)	2–53 (20.6 ± 11.2)	
Febrile seizures F/M/T n (%)	19/17/36 (79/57/67)	28/12/40 (74/55/67)	47/29/76 (76/56/67)	0.97 (0.03)*
STCG F/M/T n (%)	12/18/30 (50/60/55)	18/16/34 (47/72/56)	30/34/64 (48/65/56)	0.9(0.07)*
Electroclinical pattern				
F/M/T n (%)	24/29/53	34/21/55	58/50/108	0.03
Mesial	7/3/10 (29/10/19)	8/6/14 (24/29/25)	15/9/24 (26/18/22)	
AML	10/18/28 (42/62/53)	22/15/37 (65/71/67)	32/33/65 (55/66/60)	
WML	4/5/9 (17/17/17)	4/0/4 (12/0/7)	8/5/13 (14/10/12)	
BT	3/3/6 (12/10/11)	–	3/3/6 (5/6/6)	
Seizure frequency (mean/ month ± SD)				
Female	9.6 ± 7.5	9.0 ± 7.6	9.2 ± 7.5	0.46(0.03)*
Male	5.7 ± 5.6	7.2 ± 7	6.3 ± 6.1	
Total	7.4 ± 6.7	8.4 ± 7.4	7.9 ± 7	
Surgical outcome				
F/M/T n (%)	23/23/46	30/20/50	53/43/96	0.29
Seizure-free	19/22/41 (83/96/89)	26/18/44 (87/90/88)	45/40/85 (85/93/88)	

F, female; M, male; T, total; RHS, right hippocampal sclerosis; LHS, left hippocampal sclerosis; STCG, secondary tonic–clonic generalization; AML, anterior mesial lateral; WML, widespread mesial lateral; BT, bitemporal; AED, antiepileptic drugs. The first p-value is given for comparison between RHS and LHS, the second value (in parentheses)* for comparison between male and female patients.

a quiet and dimly lit environment and were carefully monitored for movements and seizure occurrence. None of them had a seizure during the procedure. ^{18}F-FDG was injected intravenously at a mean dose of 148 MBq. A summed image corresponding to the attenuation using ^{68}Ga ± ^{68}Ge transmission scans and decay-corrected uptake of ^{18}F-FDG expressed in activity concentration (Bq/ml) was obtained from two three-dimensional (3D) time frames (10 min each) collected 30–50 min after intravenous injection of the radioligand. 3D-MRI studies were acquired on a 1.5 Tesla GE-Signa scanner (General Electrics Medical Systems, Milwaukee, WI, U.S.A.) using a T_1-weighted SPGR sequence (124 contiguous slices, 1.2 mm thick; field of view 24 cm; 256 × 256 matrix; voxel size: 0.94 × 0.94 × 1.3 mm^3). Coronal T_2-weighted and fluid-attenuated inversion recovery (FLAIR) sequences (perpendicular to the hippocampal plane) were performed in all patients. MR images performed on another scan (eight cases) were not included in the statistical analysis.

All of the ^{18}F-FDG-PET and MR images were processed with the Statistical Parametric Mapping software package (SPM5, Wellcome Department of Cognitive Neurology, London, United Kingdom; http://www.fil.ion.ucl.ac.uk/spm), implemented on Matlab (The Mathworks, Natick, MA, U.S.A.; http://www.mathworks.com). Image preprocessing was performed as previously described.[20] Voxel-based morphometry (VBM) was performed using the unified segmentation implemented in SPM5. T_1-weighted images were spatially normalized, segmented into gray and white matter, unmodulated, and smoothed with a 10-mm full-width half maximum (FWHM) isotropic Gaussian kernel. ^{18}F-FDG-PET individual scans were normalized according to a homemade template to improve spatial normalization: MR images of 25 healthy subjects were first spatially normalized using the FIL-T1 template provided within SPM; the obtained transformation matrix was used to normalize the ^{18}F-FDG-PET realigned images. The mean sum of the ^{18}F-FDG-PET images from comparison subjects was computed, providing a mean image smoothed with an 8-mm FWHM isotropic Gaussian kernel used as FDG template to normalize all subjects' images. Following spatial normalization, all images were smoothed by 8 mm. Group analysis was performed by comparison with 30 healthy

subjects (16 male; range 21- to 54-year-olds; median 35). Voxel-wise comparisons were performed using SPM5 within the framework of the general linear model (GLM). Metabolic decrease (hypometabolism) and increase (hypermetabolism) were defined as relative when compared to healthy subjects and not absolute. The spatial coordinates of the maximal hypometabolic and hypermetabolic areas were used to identify brain areas that differed significantly from the controls and approximated the anatomic regions based on the stereotaxic atlas.

Statistical analysis

Demographic and clinical data analyses were performed using Statistica Statsoft. Pearson's chi-square tests and analysis of variance/multivariate analysis of variance (ANOVA/MANOVA) were used for continuous and categorical variables in between-group comparisons. The statistical significance threshold was fixed at $p < 0.05$.

For PET and MRI analysis, ^{18}F-FDG images were entered into the GLM within SPM5. To control for global glucose uptake effects we used proportional scaling global normalization, yielding an index of regional relative to global glucose uptake (gluMI). Baseline gluMI values were compared between RHS, LHS, and healthy subjects using analysis of covariance (ANCOVA), with group as between-subject factor and age and gender as confounding covariates. Group comparisons of structural images were performed on gray matter tissues using the same method. A *t*-test was used to compare the three groups. Effects of electroclinical patterns on brain metabolism were examined separately in RHS and LHS using ANCOVAs with groups (Mesial, AML, WML, and BT) as between-subject factor and age and gender as confounding covariates. The significance threshold was set at $p < 0.001$. Cluster significance thresholds (extent threshold) were set at 10 contiguous voxels to reduce type I errors introduced by potential noise. Effects of gender were separately examined in RHS and LHS using ANCOVAs with groups (male, female) as between-subject factor and age as confounding covariate. Other clinical variables (age at epilepsy onset, epilepsy duration, seizure frequency) were tested as covariates of interest in RHS and LHS, and then separately in male and female patients on each side. All correlations were examined using ANCOVAs with a threshold of significance set at $p < 0.05$.

Results

Clinical data

Most neurologic variables were similar in RHS and LHS, except for the female/male ratio, which differed significantly between the RHS (44%) and LHS (63%) groups ($p = 0.04$) (Table 1). The AML pattern was the most frequent observed electroclinical feature in the whole population (60%). However, the distribution of each pattern differed significantly according to the lateralization, the Mesial and AML patterns being more represented in LHS, whereas the WML pattern was more represented in RHS and the BT pattern was found only in RHS. STCG could occur in 56% of the patients without lateralization or gender effect. Notably, it occurred regularly in the WML group only. The type and number of antiepileptic drugs (AEDs) (1–4, mean 2.56) and the time since the last seizure (0–120 days, mean 13) did not differ significantly between RHS and LHS.

Metabolic changes

Unilateral temporal hypometabolism ipsilateral to HS involved the hippocampus, the parahippocampal gyrus, the temporal pole, and the anterior part of the lateral cortex (Fig. 1, Table 2). Extratemporal hypometabolism included the insula, the frontal and perisylvian areas (inferior frontal gyrus, precentral operculum), and the thalamus bilaterally with an ipsilateral predominance. Lateral temporal and extratemporal involvement, especially the perisylvian areas, was more extensive in RHS than in LHS. This asymmetry persisted after the exclusion of patients with atypical hemispheric dominance for language. In addition, a relative increase of metabolism (hypermetabolism) was found bilaterally, although predominantly on the side contralateral to HS, involving the temporal, mesial frontal, and posterior areas. The topography was also asymmetric: in RHS, the contralateral temporal hypermetabolism was predominant in the lateral areas, whereas in LHS it was predominant in the mesial areas. In addition, mesial frontal involvement was predominant in LHS, whereas posterior involvement was predominant in RHS. Hypermetabolic areas were also found in white matter (WM) and cerebellum bilaterally in both RHS and LHS. Of note, areas of metabolism increase partly coincided with those involved in the default mode network (DMN).[21]

Time since last seizure did not influence the metabolic changes at the group level. However, we found a positive correlation in the ipsilateral precuneus-posterior cingulate gyrus, in both RHS and LHS, and a negative correlation with the ipsilateral and contralateral WM metabolism in temporal and extratemporal areas.

Relationship with structural abnormalities

VBM group analysis demonstrated similar findings in RHS and LHS, consisting of unilateral hippocampal gyrus atrophy associated with bilateral frontal lobe gray matter concentration (GMC) decrease (medial frontal gyrus, anterior cingulate gyrus, inferior frontal gyrus, and perisylvian areas) (Fig. 1, Table 2). The severity and extent of GMC decrease were somewhat greater in LHS than in RHS. In addition, we found a GMC increase in the parahippocampal gyrus bilaterally but predominantly on the HS side. GMC of the middle part of the cingulate gyrus ipsilateral to HS also appeared to be slightly increased. Other areas labeled GM

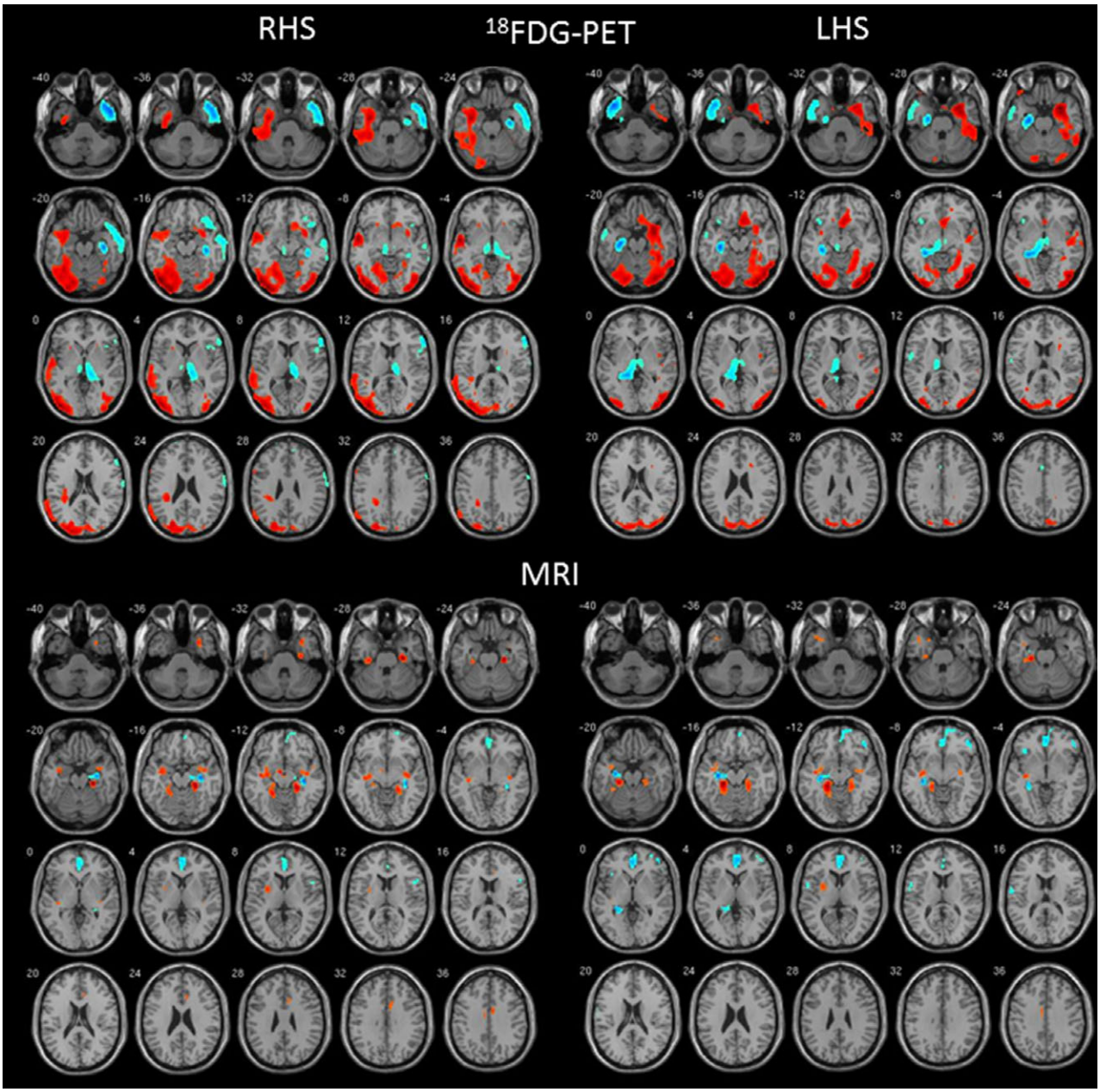

Figure 1.

Metabolic and structural changes in 54 right and 60 left hippocampal sclerosis (HS) patients and comparison with 30 healthy subjects; SPM5, $p < 0.001$. The right hemisphere is on the right side. Typical ipsilateral hypometabolism (in blue-green) involves the temporal lobe (mesial, lateral, and pole), the insular, frontal, and perisylvian areas, and the thalami (predominantly on the HS side). A larger involvement of lateral temporal and perisylvian areas is found on the right side. A relative increase of metabolism (in red) involves the contralateral temporal lobe, and the mesial frontal and the posterior areas bilaterally. Note the partial concordance between the hypermetabolic areas and the default mode network (DMN) composed of medial prefrontal and medial, lateral, inferior parietal cortices, precuneus, and cerebellum. Voxel-based morphometry demonstrated similar hippocampal atrophy (in green) on both sides and a frontoinsular gray matter concentration (GMC) decrease that is more diffuse in the left HS (LHS). Note the striking bilateral GMC increase in the parahippocampal gyri, predominantly on the HS side.

were found in the putamen, the WM of the ipsilateral temporal pole, and bilaterally in the periinsular areas. All these GMC changes were unrelated to the topography of metabolic changes.

Relationship with electroclinical patterns

A mesial temporal hypometabolism, associated with a temporal pole and bilateral thalamic hypometabolism, was similarly found in the Mesial, AML, and WML groups

Epilepsia, **(*):1–13, 2016
doi: 10.1111/epi.13377

Table 2. Metabolic and structural changes, statistical maps, and spatial coordinates (Montreal Neurological Institute space) in patients with right and left hippocampal sclerosis (HS)

	RHS (n = 54)							LHS (n = 60)						
Metabolic and structural changes	Cluster level	Voxel level T	Voxel level Z	Coordinates			Brain areas	Cluster level	Voxel level T	Voxel level Z	Coordinates			Brain areas
Hypometabolism	9,261	8.76	7.78	46	8	−42	R TP	2,493	8.48	7.59	−40	10	−40	L TP
	–	8.21	7.40	36	−22	−18	R HG	3,768	8.43	7.56	−32	−26	−16	L HG
	–	6.85	6.34	62	−10	−28	R ITG	–	5.05	4.83	−6	−14	8	L Thal
	–	6.55	6.10	60	30	14	R IFG	–	4.69	4.51	8	−14	−4	R Thal
	–	6.47	6.04	14	−28	2	R Thal.	–	3.51	3.43	−60	−24	−10	L MTG
	–	6.23	5.84	66	−8	−18	R MTG	272	4.86	4.66	−36	20	−10	L Insula
	–	5.50	5.22	36	32	−16	R OFG	226	4.72	4.54	−6	−14	58	L MFG
	–	5.16	5.92	−6	−22	−6	L Thal	256	4.57	4.40	−56	−6	12	L PrCG
	–	4.67	4.49	52	14	10	R PrCG	189	4.31	4.17	−2	14	34	L ACG
	–	4.29	4.15	4	20	40	R Insula							
	370	4.88	4.68	10	−4	48	R MFG							
	–	3.42	3.35	6	4	42	R ACG							
Hypermetabolism	24,757	7.94	7.20	−44	−80	−14	L FusG	21,709	7.67	7.00	48	−80	−8	R IOG
	–	7.94	7.20	−32	−92	−14	L IOG	–	7.48	6.84	30	6	−24	R Unc
	–	7.41	6.79	−56	−4	−6	L STG a	–	6.60	6.15	−30	−92	−12	L IOG
	–	7.13	6.57	−34	−4	−26	L Unc	–	6.30	5.90	−14	22	10	L OFG
	–	6.56	6.11	46	−78	−8	R IOG	–	5.35	5.09	28	−52	−12	R FusG
	–	6.30	5.90	−18	−82	−20	L Cereb	–	7.01	6.48	−18	−84	−18	L Cereb
	–	6.21	5.82	−22	−80	24	L Cu	–	6.47	6.04	40	−44	−22	R Cereb
	–	5.19	4.95	−22	−44	34	L PreCu	–	6.30	5.90	10	22	−14	R OFG
	–	4.87	4.67	10	−88	18	R Cu	–	5.16	4.93	−10	−92	24	L Cu
	–	4.67	4.49	30	−52	−6	RFuG	–	5.12	4.89	10	−86	32	R Cu
	–	4.54	4.38	40	−46	−22	R Cereb	–	4.95	4.74	50	14	−6	R MTG
	–	5.53	5.25	−62	−56	18	L STG p	–	4.70	4.52	−28	−64	14	L PreCU
	1,020	5.60	5.31	32	6	−14	R OFG							
	230	4.50	4.34	−22	22	−4	L ACG							
GMC decrease	301	7.4	6.74	36	−26	−10	R HG	420	7.00	6.42	−30	−16	−18	L HG
	431	5.51	5.25	0	54	4	MFG	771	5.83	5.48	6	52	6	R MFG
	–	5.04	4.80	4	44	4	R ACG	–	5.53	5.22	0	46	0	ACG
	49	4.49	4.31	54	16	14	R IFG	190	5.12	4.87	48	40	−6	R IFG
	76	4.02	3.89	16	−4	−10	R MFG	50	4.13	4.00	−38	26	−4	L Ins
	53	3.88	3.77	−36	24	−2	L IFG	90	4.06	3.93	−62	−8	16	LPoCG
								–	3.92	3.80	−56	4	10	L PrCG
GMC increase	496	7.78	7.02	28	−22	−26	R PHG	608	7.91	7.12	−20	−34	−14	L PHG
	211	5.44	5.15	−20	−44	−12	L PHG	233	5.18	4.92	24	−38	−14	R PHG
	332	5.03	4.79	−40	−14	−12	L TWM	326	4.74	4.54	−42	−10	−14	L TWM
	248	4.78	4.57	42	−10	−12	R TWM	62	4.34	4.18	−28	2	8	L Pu
	78	4.51	4.33	−28	2	8	L Pu	51	3.95	3.82	−8	−2	38	L CG
	58	4.50	4.32	−10	−8	40	L CG	58	3.74	3.63	32	−12	−10	R GH
	130	4.14	4.00	6	0	36	R CG	–	3.64	3.55	42	−10	−12	R TWM

Comparison with 30 healthy subjects, $p < 0.001$, extended voxel = 10.

R, right; L, left; a, anterior; p, posterior; ACG, anterior cingulate gyrus; CG, cingulate gyrus; Cereb, cerebellum; Cu, cuneus; FusG, fusiform gyrus; HG, hippocampal gyrus; Ins, insula; IFG, inferior frontal gyrus; IOG, inferior occipital gyrus; ITG, inferior temporal gyrus; MFG, medial frontal gyrus; MTG, middle temporal gyrus; OFG, orbitofrontal gyrus; PHG, parahippocampal gyrus; PoCG, postcentral gyrus; PrCG, precentral gyrus; PreCu, precuneus; Pu, putamen; SFG, superior frontal gyrus; STG, superior temporal gyrus; TP, temporal pole; Thal, thalamus; TWM, temporal white matter; Unc, uncus.

(Fig. 2, Table 3). As expected, we observed the most focal hypometabolism in the Mesial group and a progressive involvement of lateral temporal and extratemporal areas in the AML and WML groups. Perisylvian involvement was larger in RHS than in LHS in the WML group, accounting for the lateralization effect at the whole group level. Posterior and contralateral hypermetabolism consisted of a mirror involvement: the greater the ipsilateral hypometabolism, the greater the contralateral hypermetabolism. The BT group differed from the other groups by a limited ipsilateral hypometabolism, and the presence of a mild contralateral temporal hypometabolism and a very limited posterior hypermetabolism.

Relationship with gender

The main effect related to gender was found in the contralateral hemisphere (Fig. 3). In RHS, the metabolism was higher in female than in male patients in the left frontal lobe

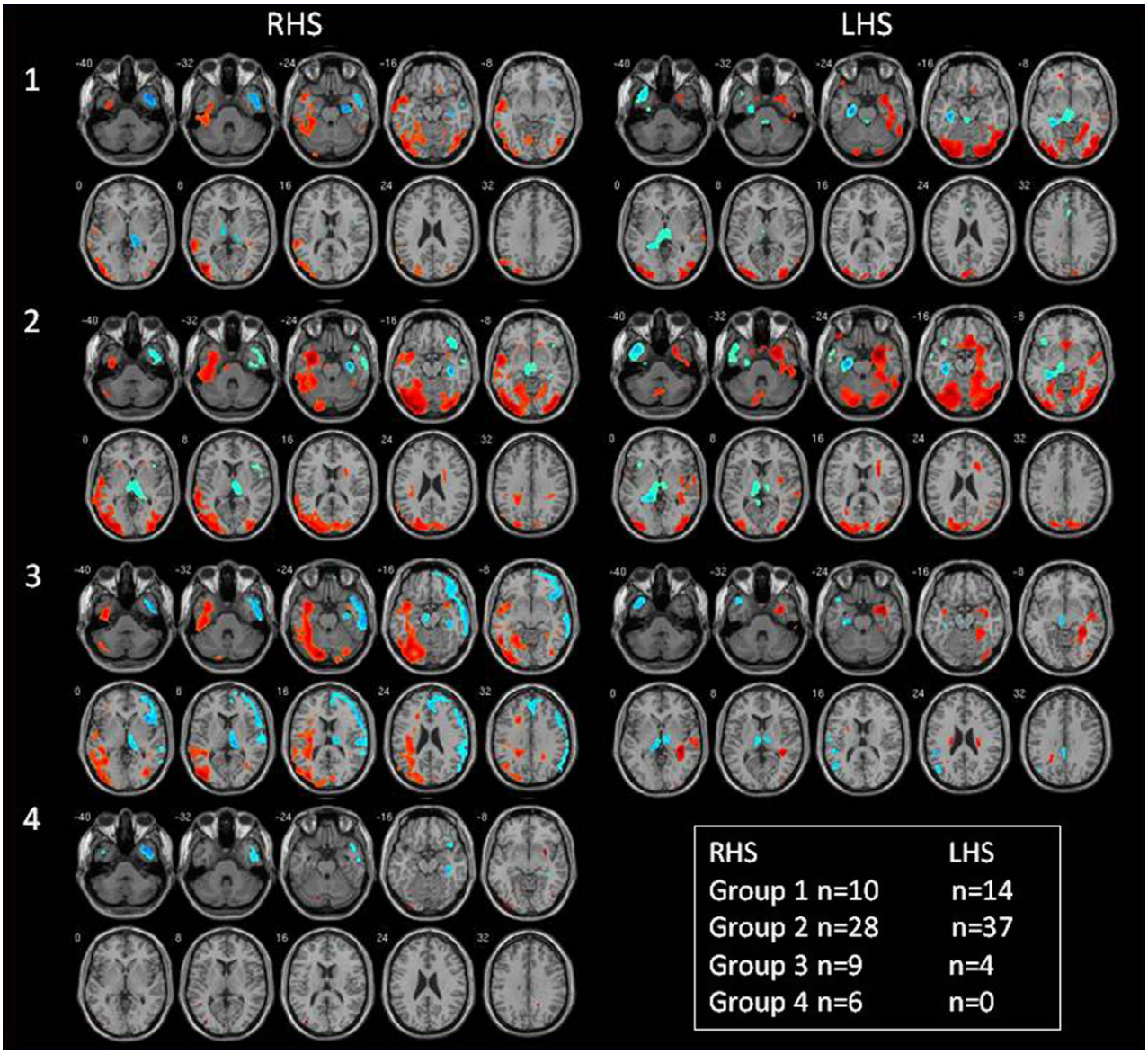

Figure 2.

Metabolic changes according to electroclinical patterns. Comparison of each group (1 = mesial, 2 = anterior mesial lateral [AML], 3 = widespread mesial lateral [WML], and 4 = bitemporal [BT]) in RHS and LHS with 30 healthy subjects; SPM5, $p < 0.001$ (right hemisphere on the right). Note the progressive hypometabolic involvement (in blue-green) of the insuloperisylvian regions from the more focal (Mesial group) to the larger epileptic networks (WML group) in both RHS and LHS, except in the BT group, in which hypometabolism is also found on the contralateral side. Perisylvian involvement is clearly larger in RHS, accounting for right and left asymmetry observed in the whole population. Hypermetabolism (in red), found in contralateral and posterior areas, is grossly proportional to the volume of the hypometabolic areas but remarkably mild in the BT group.

Table 3. Hypometabolism and hypermetabolism according to the electroclinical patterns in right and left hippocampal sclerosis (RHS and LHS)

RHS Patterns	Cluster level	Voxel level	Coordinates			Brain areas	LHS patterns	Cluster level	Voxel level	Coordinates			Brain areas
Mesial n = 10	1,022	5.27	42	8	−38	R TP	Mesial n = 14	2,390	7.41	−26	−16	−24	L HG
Hypometabolism	225	4.84	34	−18	−20	R HG	Hypometabolism	–	5.52	−8	−28	−6	L Thal
	433	4.57	14	−28	−2	R Thal		–	4.23	6	−18	−2	R Thal
	194	4.30	16	−4	50	R CG		626	5.70	−38	−14	−40	L TP
	108	3.81	−10	−14	12	L Tha		295	3.95	−4	22	42	L ACG
Hypermetabolism	5,401	6.86	−42	−82	8	L MOG	Hypermetabolism	4,716	6.64	34	−92	−12	R IOG
	–	6.19	−46	−78	−16	L FuG		–	5.67	48	−76	−6	R MOG
	–	5.38	−32	−36	−26	L ITG		–	5.55	54	−60	−18	R FuG
	–	3.85	−20	−78	24	L PreCu		–	4.47	34	6	−26	R TP
	1,032	5.45	−54	2	−12	L MTG		3,130	6.50	−30	−92	−14	L IOG
	503	5.44	−62	−36	12	L STG		–	5.17	−44	−78	−14	L FuG
	848	5.32	46	−66	16	R FuG		–	5.06	36	−88	12	L Cu
								–	4.17	−12	−4	−38	L TP
AML n = 26	3,468	8.70	36	−20	−20	R HG	AML n = 37	2,564	8.04	−32	−24	−18	L HG
Hypometabolism	–	5.33	48	0	−38	R TP	Hypometabolism	–	4.59	−8	−16	10	L Thal
	–	5.12	8	−16	10	R Thal		–	4.05	8	−14	−2	R Thal
	–	5.01	44	24	−14	R Ins/IFG		14,28	6.96	−38	10	−40	L TP
								268	4.67	−36	22	−8	L Ins
Hypermetabolism	18,029	7.50	−46	−78	−14	L FuG/IOG	Hypermetabolism	16,285	7.10	32	0	−24	R TP
	–	7.28	−36	−2	−26	L HG		–	6.31	−18	−82	−20	L Cereb
	–	6.21	−62	−32	10	L STG		–	6.14	34	−92	−12	R IOG
	–	6.08	34	−90	−12	R IOG		–	4.57	−20	−84	30	L Cu
	–	4.86	−22	−80	24	L PreCu		972	4.82	62	−4	64	R MTG
	482	4.54	−24	−40	34	L post WM		140	4.69	44	−42	−50	R Cereb
	322	4.06	28	6	18	R ant WM		121	4.02	66	−30	8	R STG
WML n = 9	10,567	6.21	40	22	−2	R Ins	WML n = 4	154	5.56	−48	−38	20	L STG post
Hypometabolism	–	5.73	58	28	14	R IFG	Hypometabolism	728	4.31	−4	−20	−6	L Thal
	–	5.48	52	−2	−36	R TP		–	4.18	8	−12	6	R Thal
	–	4.94	6	44	24	R ACG		480	4.30	−42	10	−38	L TP
	718	5.72	14	−20	12	R Thal		287	4.15	−48	−62	16	L MTG post
	241	5.07	38	−30	14	R HG		143	4.08	−30	−22	−20	L HG
Hypermetabolism	15,105	7.25	−14	−84	−22	L Cereb		103	3.96	0	−34	34	L CG post
	–	6.53	−34	−56	−2	L post WM	Hypermetabolism	2,485	6.06	40	−38	4	R FuG
	–	6.31	−48	−78	8	L MOG		–	5.60	32	−38	−6	R WM
	–	5.89	−34	−92	−10	L IOG		–	5.55	34	0	−26	R HG
	–	5.83	−36	−2	−26	L MTG		131	4.22	−24	−52	30	L WM
	–	5.14	−22	−42	32	L PreCu		–	3.81	−22	−44	34	L PreCu
	268	5.00	−20	18	32	L ant WM		88	4.10	−20	−18	22	L WM
	403	4.87	34	−78	−22	R Cereb		93	3.95	28	−22	24	R WM
	116	4.19	10	−86	16	R MOG		156	3.74	36	−94	−18	R IOG
	171	4.13	48	−44	−6	R post WM							
Bitemporal n = 6	995	5.64	36	8	−42	R TP							

Continued

Epilepsia, **(*):1–13, 2016
doi: 10.1111/epi.13377

Table 3. Continued.

RHS Patterns	Cluster level	Voxel level	Coordinates			Brain areas	LHS patterns	Cluster level	Voxel level	Coordinates	Brain areas
Hypometabolism	155	4.90	40	−30	−16	R HG					
	17	3.77	−38	4	−40	L TP					
	19	3.64	12	46	12	R ACG					
Hypermetabolism	110	4.10	−32	−94	−12	L IOG					

MNI space coordinates and brain localization (SPM5, $p < 0.001$).
R, right; L, left; ant, anterior; post, posterior; ACG, anterior cingulate gyrus; CG, cingulate gyrus; Cereb, cerebellum; Cu, cuneus; FusG, fusiform gyrus; HG, hippocampal gyrus; Ins, insula; IFG, inferior frontal gyrus; IOG, inferior occipital gyrus; ITG, inferior temporal gyrus; MOG, middle occipital gyrus; MTG, middle temporal gyrus; PreCu, precuneus; OFG, orbitofrontal gyrus; STG, superior temporal gyrus; Thal, thalamus; TP, temporal pole; WM, white matter.

($p < 0.001$) and the posterior areas (left precuneus, inferior parietal lobule, occipital lobe, and right cuneus, $p < 0.001$); in LHS, metabolism was higher in female than in male patients in the right frontal lobe ($p < 0.001$), whereas it was lower in the left cerebellum ($p = 0.009$) and the fusiform gyri bilaterally ($p = 0.021$). Regarding structural changes (not shown), GMC in RHS was higher in female than in male patients in occipital areas bilaterally, the right cerebellum ($p < 0.001$), and the right frontal lobe ($p = 0.03$), whereas it was slightly lower in the right temporal lobe (parahippocampal gyrus, $p = 0.02$). In LHS, GMC was higher in female than in male patients in the cerebellum bilaterally ($p < 0.001$) and in the right mesial frontal lobe ($p = 0.009$), whereas it was lower in the left temporal lobe (superior temporal gyrus, $p = 0.03$) and the right temporal lobe (uncus, $p = 0.004$). Overall, metabolic changes according to gender did not clearly match with GMC changes.

Relationship with epilepsy duration and age at onset

We did not find a significant correlation between epilepsy duration and the ipsilateral temporal metabolism, but there was a significant correlation with the contralateral metabolism, which differed according to the HS side (Fig. 3). In RHS, we found a negative correlation with the left temporal metabolism (inferior temporal gyrus, uncus, $p = 0.015$). We also found a negative correlation in the cerebellum ($p < 0.038$) and a positive correlation in the right anterior cingulate ($p = 0.037$). In LHS, we found a strong positive correlation with the right temporal metabolism (hippocampus and parahippocampal gyrus, $p = 0.002$) and the mesial frontal gyrus ($p = 0.027$), but no significant negative correlation. In other words, the longer the epilepsy duration, the lower the contralateral temporal metabolism in RHS and the higher it was in LHS. However, it should be noted that few patients had relatively short epilepsy duration (<10 years in only eight RHS and nine LHS patients).

Correlations between brain metabolism and age at epilepsy onset in RHS showed results opposite to those obtained with epilepsy duration. Similar results were observed in LHS; however, negative correlations were also found in the left hippocampus, in which the metabolism was lower in late-onset epilepsy and in periventricular WM bilaterally.

Relationship with seizure frequency, STGC, and number of AEDs

In RHS, we found a weak positive correlation between seizure frequency and contralateral posterior metabolism ($p = 0.036$) and no significant negative correlation (Fig. 3). In LHS, we found a positive correlation with the ipsilateral occipital ($p = 0.018$) and cerebellar metabolism ($p = 0.03$) and a negative correlation with the right temporal and frontal metabolism ($p = 0.009$). High seizure frequency

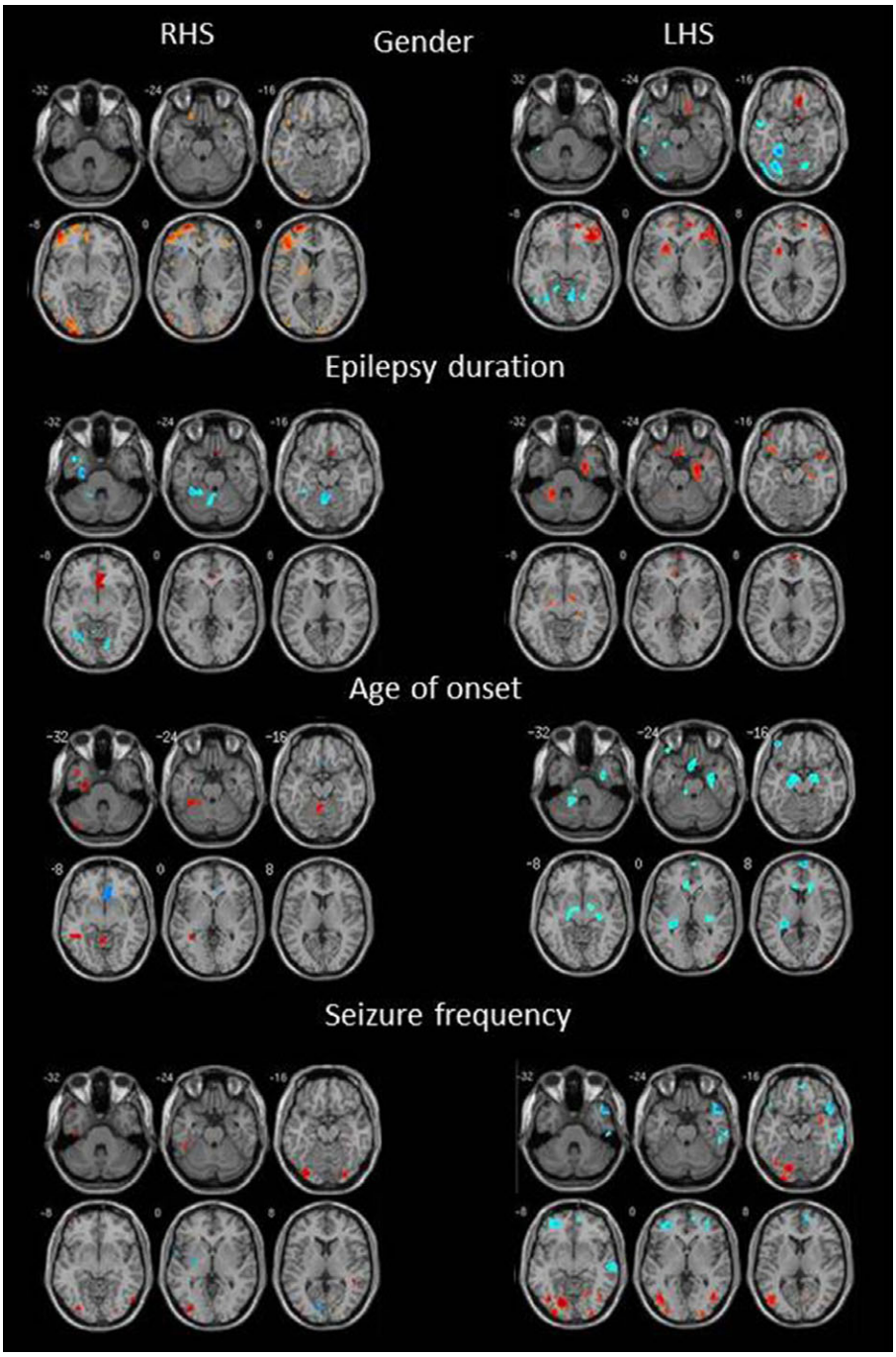

Figure 3.
Correlations between metabolism and gender, epilepsy duration, age at onset, and seizure frequency; SPM5, $p < 0.01$ (right hemisphere on the right, negative correlations in blue/green, positive correlations in orange/red). The main gender-related effect is found in the contralateral hemisphere: in RHS, the contralateral frontal and posterior metabolism is significantly higher in female than in male patients. In LHS, the right frontal lobe metabolism is higher in female patients. Note that in female patients, ipsilateral metabolism is lower in LHS. Effect of epilepsy duration is opposite on the right and left sides: in RHS, it consists of a negative correlation in the left temporal lobe and a positive correlation in the right anterior cingulate gyrus. In LHS, a positive correlation is found in the right hippocampus. Effect of age at onset shows inverse results. In LHS, additional negative correlations are found in the left hippocampus and in periventricular white matter bilaterally. Effect of seizure frequency is predominantly found in LHS, with a negative correlation in the right temporal and frontal lobes and a positive correlation in posterior areas.

therefore had a greater effect on the left hemisphere than on the right.

We observed a trend for a more extensive extratemporal hypometabolism in patients with compared to those without STCG; however, the difference was significant only in RHS for the group with frequent STCG compared with the group without STCG. For this contrast, we found a significant hypometabolism in the ipsilateral anterior cingulate gyrus ($p = 0.043$). In addition, we found a positive correlation between the number of AEDs and the metabolism in WM (ipsilateral temporal in RHS, posterior bilateral in LHS), and a negative correlation in the right thalamus in RHS and in bilateral putamen in LHS.

Discussion

Based on a large cohort of patients with MTLE, we demonstrated that the main determinant of hypometabolism ipsilateral to HS was the extent of epileptic networks, as assessed by electroclinical correlations. We found a

hemispheric asymmetry, mainly affecting the perisylvian areas, which were more extensively involved in RHS. In addition, contralateral temporal hypometabolism was only found on the right side. This discrepancy cannot be related to a selection bias, since all consecutive patients with HS were enrolled in the study, without priori consideration of the clinical features. Structural abnormalities were somewhat greater in LHS and therefore cannot explain the metabolic asymmetry. Gender, epilepsy duration, age at onset, and seizure frequency all contributed to some intergroup differences; however, none of these factors appears to account for the variability of ipsilateral hypometabolism. A second important finding is the highlighting of a contralateral and posterior hypermetabolism grossly proportional to hypometabolism, the mechanisms of which deserve attention.

Asymmetry of hypometabolism between RHS and LHS

Few studies have investigated metabolic asymmetry in MTLE, since most of them (including our previous studies)[4,5] summed both hemispheres by flipping one side on the other side.[22–25] Our present data point to the importance of studying each hemisphere separately when considering the effect of any clinical variable on brain metabolism.

The larger involvement of the right hemisphere appears in contradiction with previous series that reported a more severe hypometabolism on the left side, especially in the frontal lobe.[2,17,19] This asymmetry was associated primarily with a history of STCG and related to the spread of ictal discharges in extratemporal areas.[18] This partial disagreement may be explained by differences in methodology (mainly based on preselected ROI) and in patient selection. Notably, the occurrence of STCG appears insufficient to identify the different pathways of propagation, since it can be observed from the more focal to the larger epileptic networks. However, further studies are needed to confirm this discrepancy.

Effect of structural alterations

We found GMC decrease in mesial temporal and extratemporal areas, especially in the frontal lobes, with a slight predominance in LHS. These results are in agreement with most previous studies reporting more diffuse alterations on the left side.[14–16] The vulnerability of the left hemisphere, in relationship to the specialization for language, may account for these data. Another intriguing finding is the bilateral GMC increase found in the parahippocampal and cingulate gyri, which has also been reported by others and is considered to reflect blurring of gray–white matter demarcation due to subcortical gliosis or microdysgenesis.[14] Nevertheless, this GMC increase cannot interfere with the topography of metabolic changes, since they were observed symmetrically on both sides. The discordance between structural and metabolic data remains challenging. Because both modalities are difficult to investigate on a large scale and in homogeneous pathologies, further studies using multimodal imaging are required to investigate this issue.

Effect of gender

Recent interest has focused on gender-related effects on epilepsy susceptibility and consequences, which could result from brain development and maturation dissimilarity.[26] Large cohorts of healthy subjects have demonstrated the sexual dimorphism of the human brain[27] and the susceptibility to aging effects of the left hemisphere in men.[28] Despite some electroclinical variability between male and female patients, we did not find any significant differences according to gender. More frequent STCG in male patients[29] was not confirmed in our population as in another study.[30] With respect to the PET results, the main effect was a higher contralateral metabolism in female patients, especially in the frontal lobe. We cannot confirm the gender effect on ipsilateral hypometabolism reported previously[18,19]; however, our results suggest that compensatory mechanisms could be more efficient in female than in male patients.

Effect of epilepsy duration, age at onset, and seizure frequency

Considering MTLE as a progressive disorder, our data provide contrasted information with distinct levels of impact on ipsilateral and contralateral metabolism according to the side. We found no relationship between the ipsilateral hypometabolism and epilepsy duration. However, we found a negative correlation with the contralateral temporal metabolism in RHS. This result is in line with those of previous studies demonstrating that bitemporal hypometabolism correlated with the duration of epilepsy.[4,11,12] Furthermore, we found an opposite effect in LHS, with a contralateral temporal hypermetabolism suggesting a progressive compensatory effect. These findings indicate that the adaptive mechanisms may differ during the course of epilepsy, appearing more efficient in LHS. This hypothesis is supported by connectivity studies showing an apparent disruption of interhemispheric hippocampal connections at an early stage of the disease, followed by "rebuilding" of the connections using aberrant networks that can differ in left and right MTLE.[31] On the other hand, we found only a bitemporal hypometabolism in the RHS-BT group in which the longest duration was observed. This finding raises the question of the limits of brain adaptation, which can be reduced when epilepsy duration exceeds a certain stage.

Correlations between metabolism and age at onset were the opposite of those found with epilepsy duration, probably because these factors varied inversely in our population. However, in LHS, the negative correlation in the ipsilateral hippocampus raises the question of an age-dependent effect. This would suggest that maintaining the left hippocampal metabolism may be more difficult when epilepsy starts late

rather than early in life. Furthermore, because the major effect related to seizure frequency was a negative correlation with the contralateral metabolism in LHS, it can be postulated that high seizure frequency may reduce the compensatory effect described previously.

Metabolism and epileptic networks

Regardless of structural changes and other clinical variables, we confirm a strong concordance between the topography of hypometabolism and the electroclinical patterns. We therefore emphasize the relevance of this categorization, in line with other studies that described distinct networks in MTLE and concordant metabolic alterations.[25,32] Our results suggest that seizures originating from the left hippocampus may have a more focal organization than those on the right side. The basis for several types of network organization and potential asymmetry in MTLE remains open to debate. In addition to individual causes, including genetic predisposition, the possibility of different HS entities as suggested by pathologic studies should be considered in the future to elucidate this intriguing question. Individual causes including genetic predisposition may account for this variability. In addition, different histopathological patterns described in HS should be considered in the future to elucidate this intriguing question.

In addition, the relationship between the metabolism and the epileptic networks remains incompletely understood. Given that metabolism overall reflects the synaptic activity including neural excitation and inhibition, impaired inhibitory synaptic activity results in decreased energy requirements and reduced glucose uptake, whereas strong inhibition increases demand for glucose to maintain brain metabolism. One hypothesis is that ictal discharges spread via the anatomic pathways, further facilitated by a lack of inhibition at this level, and sustaining the electroclinical features. Moreover, focal seizure activity is known to generate a surround inhibition, limiting the spread of ictal discharges in both temporal and spatial domains, and the speed of propagation depending on the strength of inhibition.[33] Accordingly, hypometabolism reflects the failure of inhibition processes within the epileptic networks, whereas hypermetabolism would correspond to the areas in which they are strengthened, tending to restrict the areas of epileptic activity. Despite this view not being supported by others postulating that the surrounding inhibition was corresponded to hypometabolism,[24] we suggest that hypermetabolism may reflect an inhibitory effect on seizure spread. This may account for the absence of contralateral temporal involvement in LHS, since contralateral mesial temporal hypermetabolism may limit the spread of ictal discharges from the LHS to the right side. This may also play a role in the preferential frontal and perisylvian propagation pathways, since hypermetabolism is predominant in posterior areas.

Structural and functional connectivity MTLE studies have pointed out the complex relationship between the epileptic and nonepileptic temporal lobes, as with the whole brain. All demonstrated the overall reorganization of the limbic circuitry, including both reduced and increased connectivity in different parts of the networks.[34–36] Increased connectivity is thought to represent a facilitated pathway of propagation, which may manifest even interictally and colocalize with hypometabolic areas.[37] In contrast, hypermetabolism detected in the nonepileptic lobe would reflect compensatory mechanisms and has been correlated with memory performances.[34,38] Of interest, hypermetabolism observed in posterior and contralateral areas partly coincides with areas involved in the DMN, in which alterations of functional connectivity have been demonstrated in MTLE.[21,39] Metabolic-functional correlations support the notion that subjects with higher metabolic utilization in focal brain regions will also exhibit higher connectivity.[40] However, given that most areas of metabolic increase coincide with those involved in the DMN, our findings rather suggest a disruption between metabolic and functional connectivity in these networks.

New concepts in MTLE are progressively emerging from the integration of multimodal imaging data. In the addition to the evidence to support a progressive disease, the network reorganization of limbic circuitry and the interactions with global brain connectivity have been highlighted by convergent studies. Brain plasticity tends to limit the consequences of recurrent seizures to some degree. Lateralization of the epileptogenic lesion, gender, duration of epilepsy, age at onset, and seizure frequency all play a role in these adaptive changes. However, despite the influence of several variables that need to be considered when interpreting ^{18}F-FDG-PET, hypometabolism reflects mainly the extent of epileptic networks, providing a reliable noninvasive map for surgery.

Acknowledgments

The authors thank Drs. Baris Turak and Michael Mann for their participation in patients' clinical care and the team of SHFJ, especially Patrick Bodilis, Christine Baron, Brigitte Jouve, Vincent Brulon, Thierry Lekieffre, and Fabien Rastello, for their technical assistance with PET scans.

Additional Contributors

All authors were involved in drafting and revising the article.

Disclosure

The authors have no conflicts of interest to declare. We confirm that we have read the Journal's position on issues involved in ethical publication and affirm that this report is consistent with those guidelines.

References

1. Engel J, Brown WJ, Kuhl DE, et al. Pathological findings underlying focal temporal lobe hypometabolism in partial epilepsy. *Ann Neurol* 1982;12:518–528.

2. Theodore WH, Fishbein D, Dubinski R. Patterns of cerebral glucose metabolism in patients with partial seizures. *Neurology* 1988;38:1201–1206.
3. Henry TR, Babb TL, Engel J, et al. Hippocampal neuronal loss and regional hypometabolism in temporal lobe epilepsy. *Ann Neurol* 1994;36:925–927.
4. Chassoux F, Semah F, Bouilleret V, et al. Metabolic changes and electro-clinical patterns in mesio-temporal lobe epilepsy: a correlative study. *Brain* 2004;127:164–174.
5. Rusu V, Chassoux F, Landré E, et al. Dystonic posturing in seizures of mesial temporal origin: electroclinical and metabolic patterns. *Neurology* 2005;65:1612–1619.
6. Engel J, Thompson PM. Going beyond hippocampocentricity in the concept of mesial temporal lobe epilepsy. *Epilepsia* 2012;53:220–233.
7. Richardson MP. Large scale brain models of epilepsy: dynamics meets connectomics. *J Neurol Neurosurg Psychiatry* 2012;83:1238–1248.
8. Bonilha L, Rorden C, Appenzeller S, et al. Gray matter atrophy associated with duration of temporal lobe epilepsy. *NeuroImage* 2006;32:1070–1079.
9. Keller SS, Schoene-Bake JC, Gerdes JS, et al. Concomitant fractional anisotropy and volumetric abnormalities in temporal lobe epilepsy: cross-sectional evidence for progressive neurologic injury. *PLoS ONE* 2012;7:e46791.
10. Bernhardt BC, Kim H, Bernasconi N. Patterns of subregional mesiotemporal disease progression in temporal lobe epilepsy. *Neurology* 2013;81:1840–1847.
11. Jokeit H, Ebner A, Arnold S, et al. Bilateral reductions of hippocampal volume, glucose metabolism, and Wada hemispheric memory performance are related to the duration of mesial temporal lobe epilepsy. *J Neurol* 1999;246:926–933.
12. Koutroumanidis M, Hennessy MJ, Seed PT, et al. Significance of interictal bilateral temporal hypometabolism in temporal lobe epilepsy. *Neurology* 2000;54:1811–1821.
13. Theodore WH, Kelley K, Toczek MT, et al. Epilepsy duration, febrile seizures, and cerebral glucose metabolism. *Epilepsia* 2004;45:276–279.
14. Keller S, Wieshmann U, Mackay C, et al. Voxel based morphometry of grey matter abnormalities in patients with medically intractable temporal lobe epilepsy: effects of side of seizure onset and epilepsy duration. *J Neurol Neurosurg Psychiatry* 2002;73:648–656.
15. Kemmotsu N, Girard H, Bernhardt B, et al. MRI analysis in temporal lobe epilepsy: cortical thinning and white matter disruptions are related to side of seizure onset. *Epilepsia* 2011;52:2257–2266.
16. Besson P, Dinkelacker V, Valabregue R, et al. Structural connectivity differences in left and right temporal lobe epilepsy. *NeuroImage* 2014;100:135–144.
17. Jokeit H, Seitz R, Markowitsch H, et al. Prefrontal asymmetric interictal glucose hypometabolism and cognitive impairment in patients with temporal lobe epilepsy. *Brain* 1997;120:2283–2294.
18. Savic I, Engel J Jr. Sex differences in patients with mesial temporal lobe epilepsy. *J Neurol Neurosurg Psychiatry* 1998;65:910–912.
19. Nickel J, Jokeit H, Wunderlich G, et al. Gender-specific differences of hypometabolism in mTLE: implication for cognitive impairments. *Epilepsia* 2003;44:1551–1561.
20. Paillère Martinot M-L, Martinot J-L, Ringuenet D, et al. Baseline brain metabolism in resistant depression and response to transcranial magnetic stimulation. *Neuropsychopharmacology* 2011;36:2710–2719.
21. Cataldi M, Avoli M, de Villers-Sidani E. Resting state networks in temporal lobe epilepsy. *Epilepsia* 2013;54:2048–2059.
22. Van Bogaert P, Massager N, Tugendhaft P, et al. Statistical parametric mapping of regional glucose metabolism in mesial temporal lobe epilepsy. *NeuroImage* 2000;12:129–138.
23. Trotta N, Goldman S, Legros B, et al. Changes in functional integration with the non-epileptic temporal lobe of patients with unilateral mesiotemporal epilepsy. *PLoS ONE* 2013;8:e67053.
24. Nelissen N, Van Paesschen W, Baete K, et al. Correlations of interictal FDG-PET metabolism and ictal SPECT perfusion changes in human temporal lobe epilepsy with hippocampal sclerosis. *NeuroImage* 2006;32:684–695.
25. Guedj E, Bonini F, Gavaret M, et al. ^{18}FDG-PET in different subtypes of temporal lobe epilepsy: SEEG validation and predictive value. *Epilepsia* 2015;56:414–421.
26. Savic I, Engel J. Structural and functional correlates of epileptogenesis – does gender matter? *Neurobiol Dis* 2014;70:69–73.
27. Feis DL, Brodersen KH, von Cramon DY, et al. Decoding gender dimorphism of the human brain using multimodal anatomical and diffusion MRI data. *NeuroImage* 2013;70:250–257.
28. Fujimoto T, Matsumoto T, Fujita S, et al. Changes in glucose metabolism due to aging and gender-related differences in the healthy human brain. *Psychiatry Res* 2008;164:58–72.
29. Janszky J, Schulz R, Janszky I, et al. Medial temporal lobe epilepsy: gender differences. *J Neurol Neurosurg Psychiatry* 2004;75:773–775.
30. Bone B, Fogarasi A, Schulz R, et al. Secondarily generalized seizures in temporal lobe epilepsy. *Epilepsia* 2012;53:817–824.
31. Morgan VL, Conrad BN, Abou-Khalil B, et al. Increasing structural atrophy and functional isolation of the temporal lobe with duration of disease in temporal lobe epilepsy. *Epilepsy Res* 2015;110:171–178.
32. Memarian N, Madsen SK, Macey PM, et al. Ictal depth EEG and MRI structural evidence for two different epileptogenic networks in mesial temporal lobe epilepsy. *PLoS ONE* 2015;10:e0123588.
33. Lemieux L, Daunizeau J, Walker MC. Concepts of connectivity and human epileptic activity. *Front Syst Neurosci* 2011;5:1–13.
34. Bettus G, Guedj E, Joyeux F, et al. Decreased basal fMRI functional connectivity in epileptogenic networks and contralateral compensatory mechanisms. *Hum Brain Mapp* 2009;30:1580–1591.
35. Bonilha L, Nesland T, Martz GU, et al. Medial temporal lobe epilepsy is associated with neuronal fibre loss and paradoxical increase in structural connectivity of limbic structures. *J Neurol Neurosurg Psychiatry* 2012;83:903–909.
36. Voets NL, Beckmann CF, Cole DM, et al. Structural substrates for resting network disruption in temporal lobe epilepsy. *Brain* 2012;135:2350–2357.
37. Maccotta L, He BJ, Snyder AZ, et al. Impaired and facilitated functional networks in temporal lobe epilepsy. *Neuroimage Clin* 2013;2:862–872.
38. Trotta N, Goldman S, Legros B, et al. Metabolic evidence for episodic memory plasticity in the nonepileptic temporal lobe of patients with mesial temporal epilepsy. *Epilepsia* 2011;52:2003–2012.
39. Zeng H, Pizarro R, Nair VA, et al. Alterations in regional homogeneity of resting-state brain activity in mesial temporal lobe epilepsy. *Epilepsia* 2013;54:658–666.
40. Nugent AC, Martinez A, D'Alfonso A, et al. The relationship between glucose metabolism, resting-state fMRI BOLD signal, and GABAA-binding potential: a preliminary study in healthy subjects and those with temporal lobe epilepsy. *J Cereb Blood Flow Metab* 2015;35:583–591.